



Proceeding Paper

Evaluation of CloudSat Products with ACTRIS Lidar/Radar Measurements over the Eastern Mediterranean [†]

Kalliopi A. Voudouri ^{1,2,*}, Eleni Marinou ¹ , Iliana Koutsoupi ^{1,3}, Maria-Elissavet Koukouli ² ,
Ioanna Tsikoudi ^{1,3} , Alessandro Battaglia ⁴ and Pavlos Kollias ⁵

¹ Institute for Astronomy, Astrophysics, Space Application and Remote Sensing (IAASARS), National Observatory of Athens, 11810 Athens, Greece; elmarinou@noa.gr (E.M.); il.koutsoupi@noa.gr (I.K.); jtsik@noa.gr (I.T.)

² Department of Physics, Aristotle University of Thessaloniki, 54124 Thessaloniki, Greece; mariliza@auth.gr

³ Department of Physics, Section of Environmental Physics-Meteorology, National and Kapodistrian University of Athens, 10679 Athens, Greece

⁴ Department of Environment, Land and Infrastructure Engineering, Politecnico di Torino, 10121 Turin, Italy; alessandro_battaglia@polito.it

⁵ School of Marine and Atmospheric Sciences, Stony Brook University, New York, NY 11794-5000, USA; pavlos.kollias@stonybrook.edu

* Correspondence: kavoudou@noa.gr

[†] Presented at the 16th International Conference on Meteorology, Climatology and Atmospheric Physics—COMECAP 2023, Athens, Greece, 25–29 September 2023.

Abstract: In this study, we evaluate NASA CloudSat products using ground-based measurements performed in the framework of the Aerosol, Clouds, and Trace Gases Research Infrastructure (ACTRIS). Combined ground-based lidar–radar observations performed in the framework of the PRE-TECT experiment during April 2017 at the Greek Atmospheric Observatory in Finokalia, Greece (35.338° N, 25.670° E, 250 m asl) are used to evaluate the CloudSat performance in detecting hydrometeors. A case study with a persistent thin high layer, mostly consisting of aspherical particles, is presented here. CloudSat CPR (Cloud Profiling Radar) observations detect the hydrometeor layer with a top higher than that detected by the collocated ground-based cloud Doppler radar system (9.0 vs. 8.4 km) and a base higher than that detected by the lidar system (7.1 vs. 6.5 km). The outcome of this work is a step towards the use of CloudSat products for performing a decade-long cloud statistical analysis over the poorly studied East Mediterranean region.

Keywords: clouds; microphysical properties; remote sensing; CloudSat



Citation: Voudouri, K.A.; Marinou, E.; Koutsoupi, I.; Koukouli, M.-E.; Tsikoudi, I.; Battaglia, A.; Kollias, P. Evaluation of CloudSat Products with ACTRIS Lidar/Radar

Measurements over the Eastern Mediterranean. *Environ. Sci. Proc.*

2023, 26, 194. <https://doi.org/10.3390/environsciproc2023026194>

Academic Editors: Konstantinos Moustiris and Panagiotis Nastos

Published: 15 September 2023



Copyright: © 2023 by the authors. Licensee MDPI, Basel, Switzerland. This article is an open access article distributed under the terms and conditions of the Creative Commons Attribution (CC BY) license (<https://creativecommons.org/licenses/by/4.0/>).

1. Introduction

Clouds play a crucial role in weather and climate, producing precipitation and impacting the Earth's radiation budget. The processes governing their formation, evolution, geometrical, and microphysical properties, as well as their radiative effects, are far from being well understood [1]. State-of-the-art methodologies use combined lidar–radar satellite observations to provide high-resolution vertical profiles of cloud properties. Combined CloudSat and CALIPSO (Cloud-Aerosol Lidar and Infrared Pathfinder Satellite Observation) observations provided global cloud geometrical and microphysical properties from 2006 to 2017 (e.g., raDAR/liDAR product (DARDAR-MASK product); [2]). However, these data have not been used to provide cloud statistics over the Mediterranean, and this is partially attributed to the lack of evaluation studies of the products above the region. In this study, we perform an evaluation of the CloudSat geometrical and microphysical products using measurements performed in the framework of the Aerosol, Clouds, and Trace Gases Research Infrastructure (ACTRIS; <https://www.actris.eu/>, accessed on 22 August 2023). The performance of CloudSat in detecting hydrometeors and its accuracy in determining the location of cloud tops and bases on a complex atmospheric scene over the Finokalia

background station, on the island of Crete, in the eastern Mediterranean, are presented and discussed.

2. Data and Methodology

2.1. Ground-Based Measurements

The ground-based data used in our study were acquired during the PRE-TECT experimental campaign [3], the first ever Cloudnet campaign that was held in Greece [4]. The campaign was organized by the National Observatory of Athens (NOA) in the framework of the ACTRIS project and the ERC (European Research Council) project “Does dust TriboElectrification affect our ClimaTe?” (D-TECT) and took place on 1–30 April 2017, at the Greek Atmospheric Observatory of Finokalia (35.338° N, 25.670° E, 250 m asl), in Crete (finokalia.chemistry.uoc.gr, accessed on 22 August 2023). Finokalia is a background station (Figure 1b), far away from anthropogenic pollution sources, and is ideal for evaluating the cloud evolution, lifetimes, and precipitation processes.

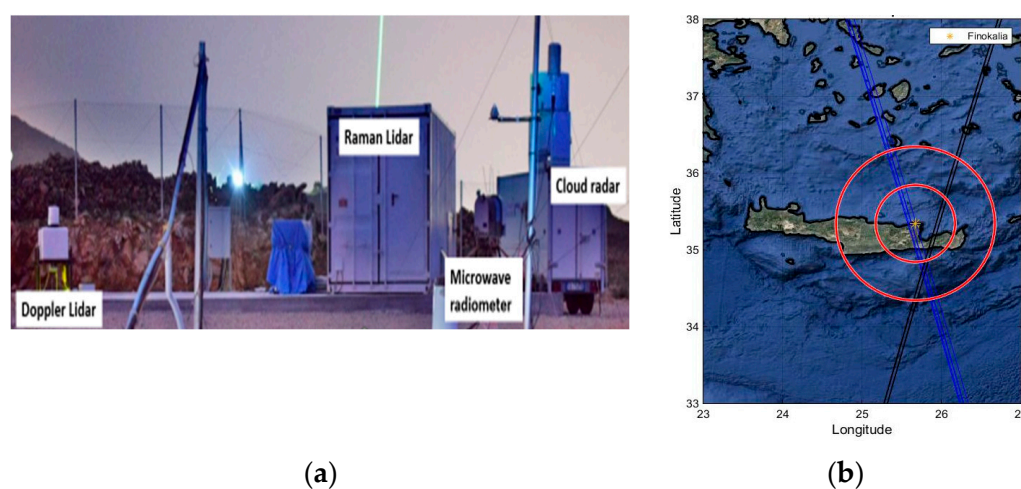


Figure 1. The PRE-TECT campaign Cloudnet station (a) and CloudSat overpass over Finokalia background station (35.338° N, 25.670° E) in Greece on 11 April 2017 (b).

During the experiment, continuous observations of aerosols, clouds, and winds were performed with high vertical and temporal resolution. We analyzed collocated measurements from the PollyXT lidar system of NOA [5], the MIRA36 cloud Doppler radar system [6] of the Italian National Research Council’s Institute of Methodologies for Environmental Analysis (CNR-IMAA), the RPG microwave radiometer of the National Research & Development Institute Optoelectronics (INOE), and the Halo Doppler wind lidar [7] of the Finnish Meteorological Institute (FMI). These instruments are shown in Figure 1a.

2.2. Satellite-Based Observations

The CloudSat cloud profiling radar (CPR) [8,9] has been operating since 2 June 2006. CloudSat flies in the A-Train constellation of satellites, along with the Cloud-Aerosol Lidar and Infrared Pathfinder Satellite Observation (CALIPSO) satellite (<https://www-calipso.larc.nasa.gov/>, accessed on 22 August 2023). CloudSat operates at 95 GHz with a sensitivity of -30 dBZ. Radar reflectivities are sampled every 240 m, with a vertical resolution of around 480 m. Profile spacing is approximately 1 km along track, with a volume resolution of 1.8 km along track and 1.5 km cross track. The A-train follows a Sun-synchronous orbit set to cross the Equator at 13:30 local time, repeating its ground track every 16 d. In this study, we use the 2B-GEOPROF (R05) radar reflectivity product [10,11] and the 2B-CLDCLASS (R05) cloud type product ([12]; <http://cloudsat.cira.colostate.edu/dataICDlist.php?go=list&path=/2B-CLDCLASS>, accessed on 22 August 2023). CloudSat provides the classification of clouds into eight categories: stratus (St), stratocumulus (Sc), cumulus (Cu), nimbostratus (Ns), altocumulus (Ac), altostratus (As), deep convective

clouds (Dc), and high-level clouds (Ci), according to their precipitation status, cloud-base height (H_{base}), cloud thickness (CTH), cloud-top height (H_{top}), cloud-top temperature, and radar reflectivity factor (Z_e).

3. Results

A case study of collocated lidar–radar ground-based and space-based observations is analyzed to retrieve the cloud properties and discuss the CloudSat performance above the eastern Mediterranean region (Figure 1b). The acquired ground-based radar and lidar observations that are used for monitoring the hydrometeors above Finokalia are shown in Figure 2 for 11 April 2017. The figure highlights the advantage of the combination of radar and lidar instruments to identify cloud boundaries and phases. The two instruments have complementary properties; the radar can penetrate even optically thick clouds and is more sensitive to large particles (i.e., raindrops and snowflakes) than the tiny cloud droplets typically formed in fog and optically thin clouds, whereas the lidar is much more sensitive to the small cloud droplets and optically thin clouds while being rapidly attenuated in optically thick clouds. In the example shown in Figure 2, the cloud radar was able to detect the entire cloud structure above the station from 13:00 to 24:00 UTC, with the vertical in-cloud extent exceeding 5 km, while the lidar was able to penetrate only the first 2 km inside the cloud. In contrast, the lidar detected thin layers with high attenuated backscatter coefficient values at altitudes between 3 and 4 km, from 06:00 to 12:00 UTC, which are not visible from the radar. The MIRA36 cloud Doppler radar system’s reflectivity values are found below the detection limit value (<-30 dBZ) until 12:00 UTC, indicating the presence of small cloud particles. The complementary observations of the PollyXT volume depolarization ratio show that the majority of the particles in these layers are nonspherical, in contrast to the surrounding targets, where spherical particles also prevail. Thus, the combined information of the ground-based lidar and radar observations indicates the coexistence of ice particles and water droplets in these layers in the presented case.

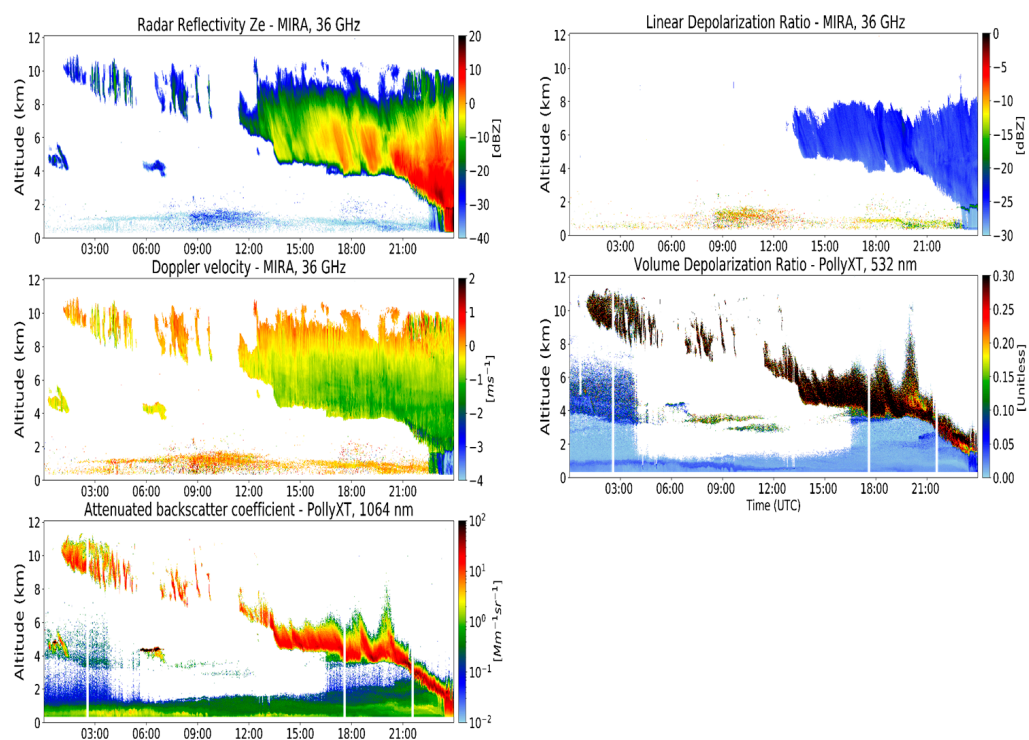


Figure 2. Observations of the radar reflectivity (upper left), radar Doppler velocity (center left), lidar attenuated backscatter coefficient (down left), MIRA linear depolarization ratio (upper right), and lidar volume depolarization ratio (down right) measured on 11 April 2017 above Finokalia, Crete.

At 10:41 UTC, CloudSat overpassed within 100 km of Finokalia station. The CloudSat radar reflectivity and the CPR Cloud mask are presented in Figure 3. In this figure, reflectivities associated with a “CPR_cloud_mask” value ≥ 30 indicate high confidence in the cloud retrieval. Cloudsat monitors a deep cloud layer located between 2.5 and 10 km inside the $2^\circ \times 2^\circ$ domain and a thinner layer above Finokalia. The ground-based radar retrievals ± 0.5 h of the overpass indicate the existence of high-level clouds, with a mean base at 7.1 ± 0.4 km and a mean top at 8.2 ± 0.35 km. The cloud boundaries are also calculated from the PollyXT by applying the wavelet covariance transform (WCT) to the 1064 nm signal, following the steps of [13]. Table 1 summarizes the geometrical boundaries of the detected cloud layers from the collocated ground-based lidar/radar measurements and the CloudSat products. CloudSat CPR observations detect the hydrometeor layer with a top higher than that detected by the collocated ground-based cloud Doppler radar system (9.0 vs. 8.4 km) and a base higher than that detected by the lidar system (7.1 vs. 6.5 km). The CALIPSO retrievals at 11:38 UTC are also presented in Figure 4. The CALIPSO Cloud Subtype also denotes the existence of aspherical particles (i.e., cirrus) over Finokalia station, while the development of deep convective clouds was also observed in the broader region.

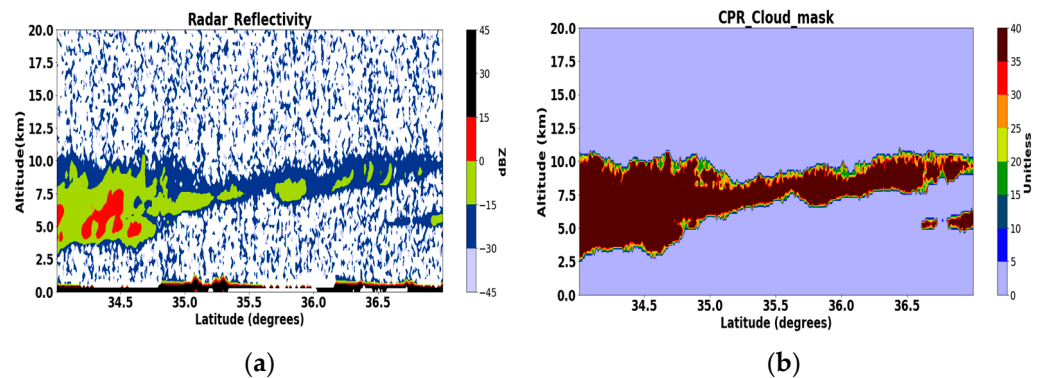


Figure 3. Radar reflectivity (a) and the CPR Cloud mask (b) of the CloudSat overpass on 11 April 2017 at 10:41 above Finokalia, Crete.

Table 1. Cloud boundaries identified by ground-based lidar/radar retrievals and CloudSat for the case study on 11 April, 2017, over Finokalia.

Instrumentation	Base	Top
MIRA36	7.2 ± 0.1 km	8.4 ± 0.35 km
PollyXT	6.5 km	8.3 km
CloudSat	7.1 ± 1.1 km	9.0 ± 1.4 km

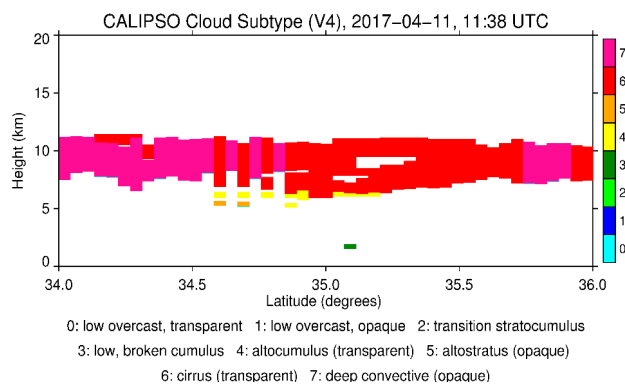


Figure 4. CALIPSO Cloud Subtype on 11 April 2017 at 11:38 above Finokalia, Crete.

The homogeneous cloud scene above Finokalia station is also depicted in Figure 5. The cloud phase flag reported by the EUMETSAT Satellite Application Facility on Climate Monitoring, CM SAF, cloud product indicates the homogeneity of the cloudy scene, with the presence of opaque clouds over Finokalia station and the existence of cirrus in the broader area on 11 April 2017 at 08:11 UTC.

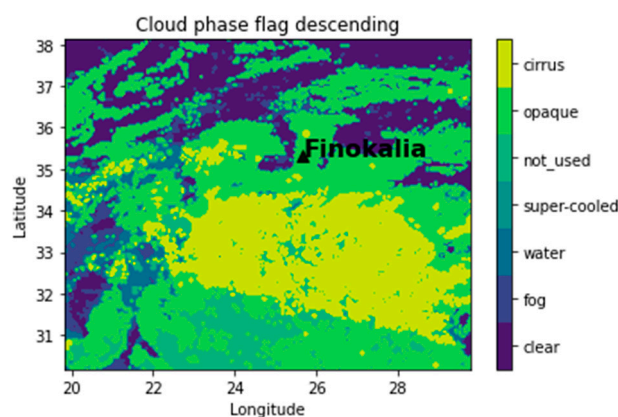


Figure 5. The cloud phase flag of the EUMETSAT CM SAF AVHRR/METOP-B v003 cloud product over the Finokalia region on 11 April 2017.

4. Conclusions

In this work, the performance of Cloudsat in monitoring a complex atmospheric scene over the background station of Finokalia in the eastern Mediterranean is presented, showing a general agreement with the ground-based instrumentation. A case study of a thin high cloud layer, mostly consisting of aspherical particles, is analyzed, and the accuracy of CloudSat in determining the location of cloud tops and bases is evaluated with the collocated ground-based lidar/radar instrumentation. The importance of accurate cloud bottom retrievals is highlighted by [14], which reports on the existing limitations and gaps in the accuracy of spaceborne radar measurements. In the future, we will extend this study by evaluating the CloudSat geometrical and microphysical products over more Mediterranean stations, combining lidar/radar retrievals. Our study is a step towards the use of CloudSat products for a decade-long cloud statistic over this under-represented region.

Author Contributions: Conceptualization, E.M., A.B. and K.A.V.; methodology, K.A.V. and E.M.; software, K.A.V., I.K., I.T. and E.M.; validation, E.M. and K.A.V.; resources, E.M.; data curation, K.A.V. and E.M.; writing—original draft preparation, K.A.V.; writing—review and editing, A.B., P.K. and M.-E.K.; visualization, K.A.V.; supervision, A.B. and E.M.; project administration, E.M.; funding acquisition, E.M. All authors have read and agreed to the published version of the manuscript.

Funding: This research was partly financially supported by PANGEA4CalVal (Grant Agreement 101079201), funded by the European Union . E.M. and I.K. acknowledge support by the Hellenic Foundation for Research and Innovation (H.F.R.I.) under the “3rd Call for H.F.R.I. Research Projects to support Post-Doctoral Researchers” (Project Acronym: REVEAL, Project Number: 07222).

Institutional Review Board Statement: Not applicable.

Informed Consent Statement: Not applicable.

Data Availability Statement: The ground-based lidar data used in this study are available upon registration at <https://polly.tropos.de/> (accessed on 5 September 2023). The ground-based cloud radar data are available upon request at <https://cloudnet.fmi.fi/> (accessed on 5 September 2023). The Cloudsat dataset is available at <https://cloudsat.atmos.colostate.edu/> (accessed on 5 September 2023). The CALIPSO dataset is available at <https://asdc.larc.nasa.gov/project/CALIPSO> (accessed on 5 September 2023). The EUMETSAT Satellite Application Facility on Climate Monitoring (CM

SAF) CPH and AVHRR/METOP-B v003 data are publicly available from <https://wui.cmsaf.eu/> (accessed on 5 September 2023).

Conflicts of Interest: The authors declare no conflict of interest.

References

1. IPCC. *Climate Change 2014: Synthesis Report. Contribution of Working Groups I, II and III to the Fifth Assessment Report of the Intergovernmental Panel on Climate Change*; Pachauri, R.K., Meyer, L.A., Eds.; IPCC: Geneva, Switzerland, 2014; p. 151.
2. Delanoë, J.; Hogan, R.J. A variational scheme for retrieving ice cloud properties from combined radar, lidar, and infrared radiometer. *J. Geophys. Res.* **2008**, *113*, D07204. [[CrossRef](#)]
3. The PRE-TECT Experimental Campaign. Available online: <http://PRE-TECT.space.noa.gr/> (accessed on 30 May 2023).
4. Marinou, E.; Voudouri, K.A.; Tsikoudi, I.; Drakaki, E.; Tsekeri, A.; Rosoldi, M.; Ene, D.; Baars, H.; O'Connor, E.; Amiridis, V.; et al. Geometrical and Microphysical Properties of Clouds Formed in the Presence of Dust above the Eastern Mediterranean. *Remote Sens.* **2021**, *13*, 5001. [[CrossRef](#)]
5. Engelmann, R.; Kanitz, T.; Baars, H.; Heese, B.; Althausen, D.; Skupin, A.; Wandinger, U.; Komppula, M.; Stachlewska, I.S.; Amiridis, V.; et al. The automated multiwavelength Raman polarization and water-vapor lidar PollyXT: The neXT generation. *Atmos. Meas. Tech.* **2016**, *9*, 1767–1784. [[CrossRef](#)]
6. Madonna, F.; Amodeo, A.; Boselli, A.; Cornacchia, C.; Cuomo, V.; D'Amico, G.; Giunta, A.; Mona, L.; Pappalardo, G. CIAO: The CNR-IMAA advanced observatory for atmospheric research. *Atmos. Meas. Tech.* **2011**, *4*, 1191–1208. [[CrossRef](#)]
7. Manninen, A.J.; O'Connor, E.J.; Vakkari, V.; Petäjä, T. A generalised background correction algorithm for a Halo Doppler lidar and its application to data from Finland. *Atmos. Meas. Tech.* **2016**, *9*, 817–827. [[CrossRef](#)]
8. Stephens, G.; Wood, N. Properties of tropical convection observed by millimeter-wave radar systems. *Mon. Weather Rev.* **2007**, *135*, 821–842. [[CrossRef](#)]
9. Stephens, G.L.; Vane, D.G.; Tanelli, S.; Im, E.; Durden, S.; Rokey, M.; Reinke, D.; Partain, P.; Mace, G.G.; Austin, R.; et al. CloudSat mission: Performance and early science after the first year of operation. *J. Geophys. Res.* **2008**, *113*, D00A18. [[CrossRef](#)]
10. Mace, G.; Marchand, R.; Zhang, Q.; Stephens, G. Global hydro-meteor occurrence as observed by CloudSat: Initial observations from summer 2006. *Geophys. Res. Lett.* **2007**, *34*, L09808. [[CrossRef](#)]
11. Marchand, R.; Mace, G.G.; Ackerman, T.; Stephens, G. Hydro-meteor detection using CloudSat an Earth-orbiting 94-GHz cloud radar. *J. Atmos. Oceanic Technol.* **2008**, *25*, 519–533. [[CrossRef](#)]
12. Sassen, K.; Wang, Z. Classifying clouds around the globe with the CloudSat radar: 1-year of results. *Geophys. Res. Lett.* **2008**, *35*, L04805. [[CrossRef](#)]
13. Voudouri, K.A.; Giannakaki, E.; Komppula, M.; Balis, D. Variability in cirrus cloud properties using a PollyXT Raman lidar over high and tropical latitudes. *Atmos. Chem. Phys.* **2020**, *20*, 4427–4444. [[CrossRef](#)]
14. Battaglia, A.; Kollias, P.; Dhillon, R.; Roy, R.; Tanelli, S.; Lamer, K.; Grecu, M.; Lebsock, M.; Watters, D.; Mroz, K.; et al. Spaceborne Cloud and Precipitation Radars: Status, Challenges, and Ways Forward. *Rev. Geophys.* **2020**, *58*, e2019RG000686. Available online: <https://hdl.handle.net/2381/13133234.v1> (accessed on 22 August 2023). [[CrossRef](#)] [[PubMed](#)]

Disclaimer/Publisher's Note: The statements, opinions and data contained in all publications are solely those of the individual author(s) and contributor(s) and not of MDPI and/or the editor(s). MDPI and/or the editor(s) disclaim responsibility for any injury to people or property resulting from any ideas, methods, instructions or products referred to in the content.